ORIENTAL JOURNAL OF CHEMISTRY
An International Open Free Access, Peer Reviewed Research Journal
www.orientjchem.org
Est. 1984
ISSN: 0970-020 X
CODEN: OJCHEG
2017, Vol. 33, No. (4):
Pg.1837-1847

QSAR Modeling, Docking and Insilico ADMET Studies of Lanosterol Synthase Inhibitors

DIVYA G NAIR[1], V.L.PUSHPA[2]* and K. KURIEN THOMAS[1]

[1]Department of Chemistry, Bishop Moore College, Mavelikara -290110, Kerala.
[2] Department of Chemistry, S N College, Kollam, Kerala.
*Corresponding author E-mail: drpushpavl@gmail.com

http://dx.doi.org/10.13005/ojc/330428

(Received: May 22, 2017; Accepted: June 24, 2017)

ABSTRACT

Lanosterol Synthase is an attractive target for antihypercholesterolemeic drug design. A set of 26 molecules having lanosterol synthase inhibitory activity was used for pharmacophoric hypothesis and atom based QSAR analysis. Inhibitory concentrations (pIC50) of these compounds were ranged from 7.452 to 8.721. Pharmacophoric hypothesis AAHPR.174 had the best survival score of 3.560. On the basis of the best hypothesis AAHPR.174, atom based 3D-QSAR validation was carried out using PLS factor, with 20 compounds in training set and 6 compounds in test set. From the regression analysis, a highly predictive and statistically significant model was generated having the co-efficient of determination (R^2 = 0.9934), cross validated co-efficient (q^2 = 0.8083), Pearson correlation co-efficient = 0.9345 and variance ratio (F = 561.9). The QSAR model indicated that hydrogen bond acceptor, aromatic, hydrophobic and positively charged groups play an important role in LSS inhibitor activities. This pharmacophoric hypothesis was used to screen ligands from Asinex database. On the basis of fitness score and docking interactions, novel ligands were selected. Insilico ADME/Toxicity predictions were analyzed to understand the lanosterol synthase inhibitor activity of these compounds and that may help in the future development of drug candidate with fewer side effects.

Keyword: Lanosterol Synthase Inhibitors, Pharmacophore, QSAR, Docking, ADME.

INTRODUCTION

Cholesterol and lipid triglycerides are essential building blocks in the structure of cells, making hormones and producing energy[1]. Hypercholesterolemia is the presence of high level of cholesterol in blood. The excess amount of cholesterol can lead to hardening and narrowing of arteries (called atherosclerosis) in the major vascular system[2]. HMG-CoA reductase Inhibitors (statin drugs) are widely used for the treatment of atherosclerosis. Long term use of statin drugs related with a reduced risk of cancer progression[3-4], elevated level of liver enzymes, kidney failure.[5] It may negatively associate with the amount of Intermediates required for other biosynthetic pathways (eg: synthesis of Isoprenoids, coenzyme Q_{10})[6-7]. Lanosterol Synthase (LSS) enzyme plays

a central role in the biosynthesis of cholesterol. In vertebrates the Lanosterol Synthase (LSS) enzyme converts (S)-2, 3-Oxidosqualene to a protosterol cation and then to a lanosterol [8-15]. Hence there is a special attention in the identification of LSS inhibitors as drugs to lower cholesterol in blood.

METHODOLOGY

Ligand preparation

A group of 26 molecules having lanosterol synthase (LSS) [EC5.4.99.7] (PDB id: 1W6J) Inhibitory activity were collected from literature survey. LSS Inhibitory activities of the molecules were changed to pIC50 values (Table 1, 2, 3 and 4)[16]. The molecules were minimized by ligprep module with semi-empirical OPLS – 2005 force field. Build and Maestro modules were used to create low energy 3D structures of the ligand.

Quantitative pharmacophore and 3D QSAR model generation

Based on the activity threshold values, the entire data set was divided into active and inactive pharmsets for generating common pharmacophore hypothesis. For actives, the activity threshold value was 8.2 and for inactives 7.6. pIC50 activity in the data set ranges from 7.452 to 8.721. Generated pharmacophore based alignment of the 3D structures of the ligand was used to derive a predictive atom based 3D QSAR model.

For generating pharmacophore model, PHASE module of Schrodinger software was used. PHASE provides default pharmacophoric features such as H-bond acceptor (A), H-bond donor (D), hydrophobic group (H), negatively charged group (N), positively charged group (P) and aromatic ring (R)[17-18]. To create 3D QSAR model, the high scored hypothesis was used.

For generating atom based QSAR model, the ligands were divided into 80% with training set (20 compounds) and 20% with test set (6 compounds) using PLS. PHASE has five PLS factors, out of which the fourth factor is found to be dominant. The quality of the generated 3D QSAR model was verified by test set predictions.

Molecular docking

Molecular docking was carried out for the validation of common pharmacophoric aspects and 3D QSAR model. Docking studies of 26 molecules were performed with the 3D structure of lanosterol synthase enzyme (PDB id: 1W6J)[19]. Protein preparation wizard panel of Schrodinger suit v9.2 was used for the preparation of protein[20]. The protein was preprocessed, optimized and minimized with force field of OPLS – 2005 and RMSD of 0.3 A^0 by protein preparation wizard[21-22]. Grid was created using the centroid of workspace ligand $R_0$48-8071.

The new ligands were screened from the fitness score in the find match to hypothesis option and docking analysis was carried out. The glide score was obtained from the favourable and unfavourable interactions of new ligands with amino acids at the active site of 1W6J protein. Based on the glide score, the best pose of the docking interaction was selected.

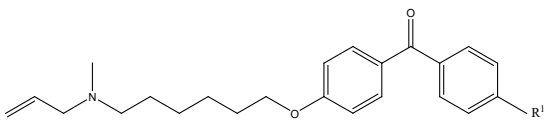

Table 1: The chemical structures of training set

Compound	R^1
1	NO_2
2	Br
3	F
4	H

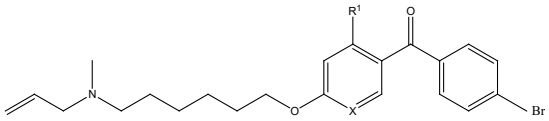

Table 2: The chemical structures of training (compounds 5- 7, 9 and 10) and test (compound 8) set

Compound	R^1	X
5	NHCH3	C
6	OCH3	C
7	SCH3	C
8	OH	C
9	F	C
10	H	N

ADME screening

Insilico ADME/Toxicity predictions were applied to understand the lanosterol synthase Inhibitor activity of the reference ligand, training set, test set and newly designed molecules. Using Qik prop module, ADME/Toxicity properties of new ligands were determined[23].

RESULTS AND DISCUSSION

To evaluate LSS enzyme – ligand interactions quantitative pharmacophore and 3D QSAR model generation methods were applied. Molecular docking was performed to elucidate the binding interactions between ligands and the lanosterol synthase enzyme. Using Qik prop module, ADME properties of molecules were analyzed.

For the formation of common pharmacophore model, the data set was split into actives (>8.2) and inactives (< 7.6). Five pointed pharmacophore hypothesis were selected and applied to scoring function analysis. The AAHPR.174 hypothesis is the best hypothesis in this analysis characterized by high survival score (3.560). The AAHPR.174 hypothesis is presented in figure 1.

The characteristics represented in this hypothesis are two hydrogen bond acceptors, one hydrophobic group, one positively charged group and an aromatic group. The best fitness score of 3 was showed by the compound sixteen and the best activity was showed by compound one having fitness score of 2.58 (figure 2a and 2b). The alignments of all active and active or inactive ligands were displayed in figure (3a) and (3b).

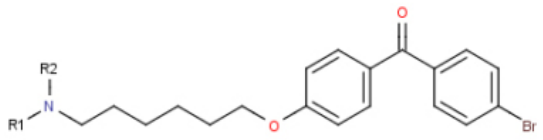

Table 3: The chemical structures of training (compounds 12 - 14) and test (compound 11) set

Compound	R1	R2
11	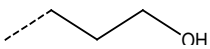	CH3
12	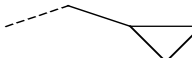	CH3
13	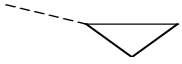	CH3
14	*H*	CH3

The hypothesis score, distance and angle between different sites of AAHPR.174 were presented in Table 5, 6 and 7. For atom based QSAR, the best AAHPR.174 hypothesis was selected. For generating 3D QSAR model, 20 ligands were taken as training set and 6 ligands were taken as test set. PLS factor four is found to have good statistics is shown in Table 8.

From the regression analysis, a highly predictive and statistically significant model was generated having the co-efficient of determination (R^2 = 0.9934), cross validated co-efficient (q^2 = 0.8083), Pearson correlation co-efficient = 0.9345 and variance ratio (F = 561.9), standard deviation of regression (SD = 0.033) and root mean squared error (RMSE = 0.09).

From the QSAR results, 95% variance was represented by the experimental and PHASE predicted pIC50 activity graph (figure 4a and 4b). The graph shows the fitting points were close to the regression line. The experimental and predicted pIC50 activities were listed in table 9. The structure and predicted pIC50 values of new ligands were presented in table 11. The new ligands showed proper predicted activity in the range of 8.088–8.290.

The reference ligand $R_0$48-8071 (Figure 5) has the glide score of -10.309 kcal/mol. The amino acids Trp 387 and Trp 581 are responsible for the cation - π interactions and Asp 455 is responsible for charged H- bond with the positive charge at the position of amino N – atom of $R_0$48-8071. The fluoro phenyl group of $R_0$48-8071 makes π-π interactions with Phe 696 and His 232. The bromo phenyl group makes π-π bonding with Trp 192.

Compound 8 (Figure 6) show the highest docking score of -14.308 kcal/mol and have interactions with Trp 581, Asp 455, His 232, Trp, 192 and Gly 380 amino acids. Highest fitness score compound 16 (Figure 7) show docking score of -9.567 kcal/mol makes interactions with Trp 581,

Table 4: The chemical structures of training (compounds 15- 20, 24 and 25) and test (compounds 21-23 and 26) set

No.	Compound M	No.	Compound M	No.	Compound M
15	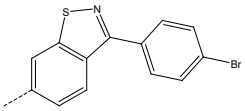	19	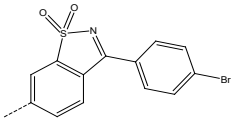	23	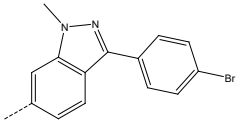
16	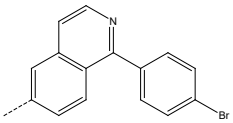	20	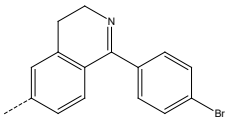	24	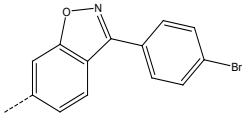
17	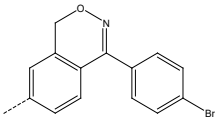	21	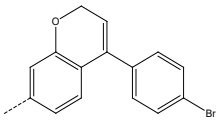	25	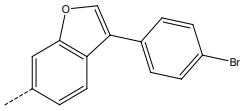
18	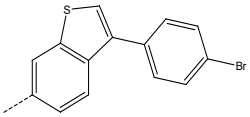	22	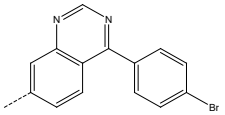	26	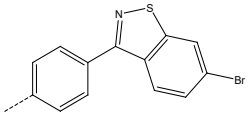

Table 5. Best three hypothesis generated

Model	Survival-Active	Survival-Inactive	Site	Vector	Volume	Activity	Inactive
AAHPR.174	3.560	1.135	0.89	0.980	0.688	8.456	2.426
AAHPR.166	3.491	1.028	0.85	0.990	0.653	8.456	2.463
AAHPR.164	3.490	0.797	0.92	0.863	0.705	8.387	2.693

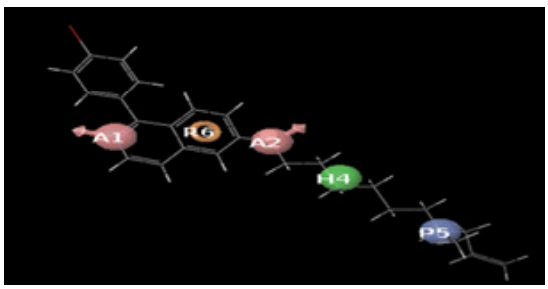

Fig.1 Formation of AAHPR .174 pharmacophore model showing two hydrogen bondacceptors (A1 and A2), one hydrophobic group (H4), one positively charged group (P5), and one aromatic ring (R6).

Table 6. Distances between different sites of model AAHPR.174

Hypothesis	Site-1	Site-2	Distance(A^0)
AAHPR.174	A1	A2	6.453
AAHPR.174	A1	H4	9.492
AAHPR.174	A1	P5	14.467
AAHPR.174	A1	R6	3.725
AAHPR.174	A2	H4	3.519
AAHPR.174	A2	P5	8.790
AAHPR.174	A2	R6	2.800
AAHPR.174	H4	P5	5.271
AAHPR.174	H4	R6	6.140
AAHPR.174	P5	R6	11.351

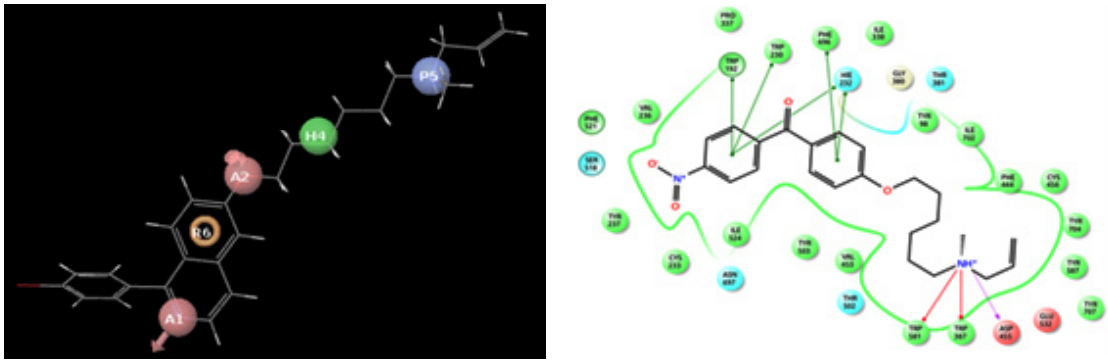

Fig. 2a: alignment of best fitness score compound 16. 2b) alignment of active Compound 1

Table 7: Angle between different sites of model AAHPR.174

Model	Site-1	Site-2	Site-3	Angle(A^0)	Model	Site-1	Site-2	Site-3	Angle(A^0)
AAHPR.174	A2	A1	H4	13.0	AAHPR.174	A1	P5	A2	15.6
AAHPR.174	A2	A1	P5	21.6	AAHPR.174	A1	P5	H4	15.5
AAHPR.174	A2	A1	R6	7.4	AAHPR.174	A1	P5	R6	9.1
AAHPR.174	H4	A1	P5	8.5	AAHPR.174	A2	P5	H4	0.5
AAHPR.174	H4	A1	R6	20.4	AAHPR.174	A2	P5	R6	6.5
AAHPR.174	P5	A1	R6	28.9	AAHPR.174	H4	P5	R6	6.4
AAHPR.174	A1	A2	H4	142.6	AAHPR.174	A1	R6	A2	162.8
AAHPR.174	A1	A2	P5	142.8	AAHPR.174	A1	R6	H4	147.4
AAHPR.174	A1	A2	R6	9.8	AAHPR.174	A1	R6	P5	141.9
AAHPR.174	H4	A2	P5	0.8	AAHPR.174	A2	P5	H4	0.5
AAHPR.174	H4	A2	R6	152.4	AAHPR.174	A2	P5	R6	6.5
AAHPR.174	P5	A2	R6	152.6	AAHPR.174	H4	P5	R6	6.4
AAHPR.174	A1	H4	A2	24.4	AAHPR.174	A1	R6	A2	162.8
AAHPR.174	A1	H4	P5	156.0	AAHPR.174	A1	R6	H4	147.4
AAHPR.174	A1	H4	R6	12.2	AAHPR.174	A1	R6	P5	141.9
AAHPR.174	A2	H4	P5	178.7	AAHPR.174	A2	R6	H4	15.4
AAHPR.174	A2	H4	R6	12.2	AAHPR.174	A2	R6	P5	20.8
AAHPR.174	P5	H4	R6	168.2	AAHPR.174	H4	R6	P5	5.5

Table 8: Statistical values for 3D QSAR model generated by PLS

Hypothesis	PLS factor	SD	R^2	F	P	Stability	RMSE	Q^2	Pearson-r
	1	0.1941	0.7286	48.3	1.7e-06	0.3461	0.12	0.6919	0.8353
	2	0.0974	0.9354	123.1	7.69e-11	-0.0679	0.07	0.8822	0.9428
AAHPR.174	3	0.0551	0.9806	269.4	6.67e-14	-0.0704	0.10	0.7964	0.9271
	4	0.0332	0.9934	561.9	3.87e-16	-0.101	0.09	0.8083	0.9345

Trp 387, Asp 455, His 232, Phe 696, Trp 192 and Trp 230.

High active compound 1 (Figure 8) show docking score of -8.880 kcal/mol and makes

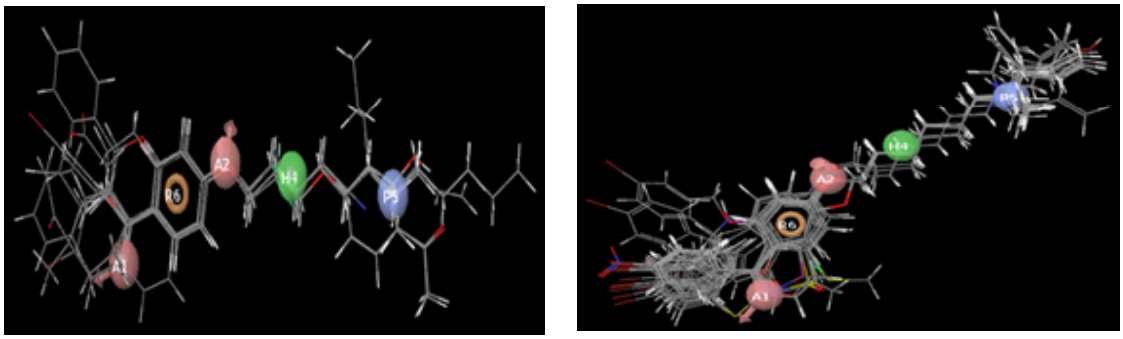

Fig.3 a) alignment of all active compounds to the pharmacophore. b) alignment of all compounds (active/inactive) to the pharmacophor

Table 9. Dataset analyzed with experimental and predicted activities.

Compound	IC50	Exp.pIC50 [nm]	Pred.pIC50	Δ	Fitness	Pharmset	Training or Test
1	1.9	8.721	8.697	0.024	2.58	Active	Training
2	5.4	8.268	8.218	0.05	2.62		Training
3	6.7	8.174	8.171	0.003	2.62		Training
4	22.5	7.648	7.623	0.025	2.64	Inactive	Training
5	4.1	8.387	8.420	-0.033	2.38	Active	Training
6	4.6	8.337	8.429	-0.092	2.44	Active	Training
7	6.2	8.208	8.229	-0.021	2.30		Training
8	6.3	8.201	8.010	0.191	2.43		Test
9	6.5	8.187	8.184	0.003	2.52		Training
10	8.7	8.060	8.015	0.045	2.55		Training
11	15.7	7.804	7.644	0.16	2.08		Test
12	31.8	7.498	7.554	0.056	2.00	Inactive	Training
13	35.3	7.452	7.509	-0.057	2.51	Inactive	Training
14	25	7.602	7.585	0.017	2.55	Inactive	Training
15	2.9	8.538	8.535	0.003	2.71	Active	Training
16	3.5	8.456	8.443	0.013	3.00	Active	Training
17	4.1	8.387	8.398	-0.011	2.69	Active	Training
18	5.6	8.252	8.250	0.002	2.46		Training
19	7.8	8.108	8.071	0.037	2.59		Training
20	7.9	8.102	8.109	-0.002	2.71		Training
21	11.4	7.943	7.932	0.011	1.22		Test
22	12.3	7.910	7.908	0.002	2.82		Test
23	19.6	7.708	7.692	0.016	2.53		Test
24	21	7.678	7.643	0.035	2.57		Training
25	14	7.854	7.850	0.004	1.29		Training
26	5	8.301	8.208	0.093	2.02		Test

Δ = (Exp.pIC50 - Pred.pIC50)

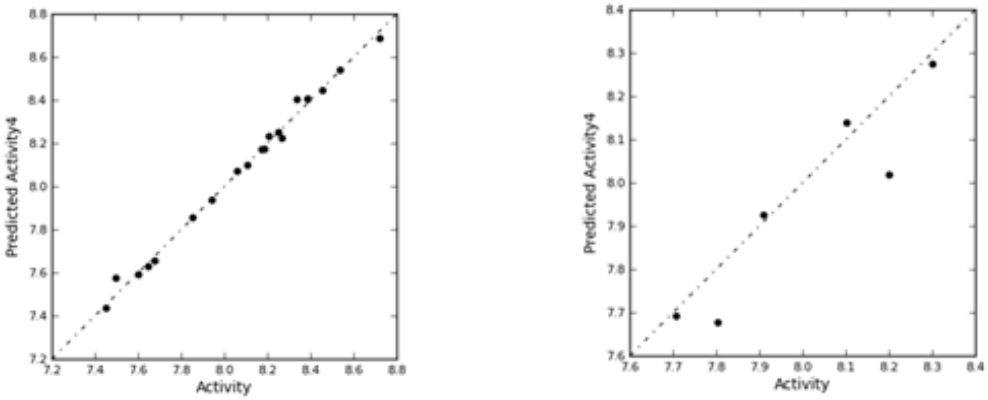

Fig. 4: Scattered plot for predicted pIC50 against experimental pIC50 for (a) training set compounds (b) test set compounds

Table 10: Docking Score and Amino acid interactions of all 26 compounds

Compound	Docking score (kcal/mol)	Amino acid interactions at the active site of 1w6j protein
1	-8.880	TRP 192, TRP 230, PHE 696, HIE 232, ASP 455, TRP 387, TRP 581.
2	-9.183	TRP 192, PHE 696, HIE 232, ASP 455, TRP 387, TRP 581.
3	-10.249	TRP 192, PHE 696, HIE 232, ASP 455, TRP 387, TRP 581.
4	-9.503	TRP 192, TRP 230, PHE 696, HIE 232, ASP 455, TRP 387, TRP 581.
5	-11.381	TRP 192, TRP 230, PHE 696, HIE 232, ASP 455, TRP 387, TRP 581.
6	-9.701	TRP 192, HIE 232, ASP 455, TRP 387, TRP 581.
7	-9.919	TRP 192, PHE 696, HIE 232, ASP 455, TRP 387, TRP 581.
8	-14.308	TRP 192, TRP 230, PHE 696, HIE 232, ASP 455, TRP 387, TRP 581.
9	-9.791	TRP 192, PHE 696, HIE 232, ASP 455, TRP 387, TRP 581.
10	-9.330	TRP 192, PHE 696, ASP 455, TRP 387, TRP 581.
11	-10.760	TRP 192, TRP 230, PHE 696, HIE 232, ASP 455, TRP 387, TRP 581.
12	-10.074	TRP 192, PHE 696, HIE 232, ASP 455, TRP 387, TRP 581.
13	-9.203	TRP 192, PHE 696, HIE 232, ASP 455, TRP 387, TRP 581.
14	-9.681	TRP 192, TRP 230, PHE 696, HIE 232, ASP 455, TRP 387, TRP 581.
15	-10.043	TRP 192, TRP 230, PHE 696, HIE 232, ASP 455, TRP 387, TRP 581.
16	-9.567	TRP 192, TRP 230, PHE 696, HIE 232, ASP 455, TRP 387, TRP 581.
17	-8.819	TRP 192, TRP 230, PHE 696, HIE 232, ASP 455, TRP 387, TRP 581.
18	-9.982	TRP 192, PHE 696, HIE 232, ASP 455, TRP 387, TRP 581.
19	-9.529	TRP 192, TRP 230, PHE 696, HIE 232, ASP 455, TRP 387, TRP 581.
20	-8.036	TRP 192, PHE 696, HIE 232, ASP 455, TRP 387, TRP 581.
21	-9.250	TRP 192, PHE 696, HIE 232, ASP 455, TRP 387, TRP 581.
22	-9.962	TRP 192, PHE 696, HIE 232, ASP 455, TRP 387, TRP 581.
23	-9.534	TRP 192, TRP 230, PHE 696, HIE 232, ASP 455, TRP 387, TRP 581.
24	-9.708	TRP 192, PHE 696, HIE 232, ASP 455, TRP 387, TRP 581.
25	-10.135	TRP 192, PHE 696, HIE 232, ASP 455, TRP 387, TRP 581.
26	-9.168	TRP 230, PHE 696, ASP 455, TRP 387, TRP 581.

A = 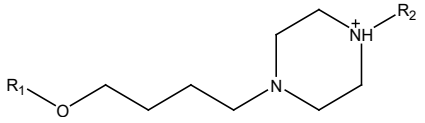

Table 11: Predicted activity, docking results and amino acid interactions of new ligands

No.	Structure		Fitness score	Predicted pIC50	Docking energy	Amino acid interactions at the active site of 1w6j protein
1	R1 = 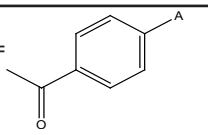	R2= -CH2-CH3	2.07	8.252	-11.853	TRP 387
2	R1 = 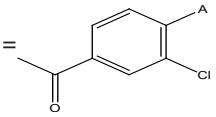	R2= -CH2-CH3	2.07	8.290	-12.575	TRP 387, ASP 455.
3	R1= 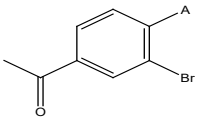	R2 = -CH2-CH3	2.39	8.274	-13.153	PHE 696, HIE 232, TYR 704, TRP 387.
4	R1 = 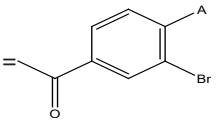	R2= -CH3	2.00	8.172	-13.223	TRP 192, PHE 444.
5	R1 = 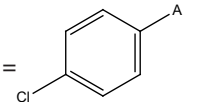	R2= -CH2-CH3	2.031	8.148	-12.358	TRP 192,TRP 581, ASP 455.
6	R1 = 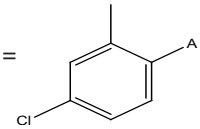	R2= -CH3	2.035	8.150	-11.620	TRP 192, PHE 444.
7	R1 = 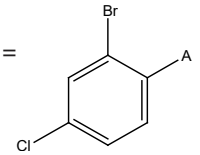	R2= -H	2.01	8.169	-11.402	TRP 230,TRP 192, PHE 444.
8	R1 = 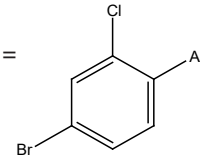	R2= -H	2.01	8.068	-11.041	TRP 230, TRP 192, PHE 444.
9	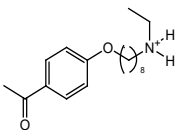		2.01	8.206	-11.735	TRP 192, TRP 387, TRP 581.
10	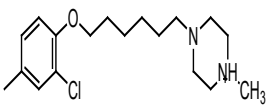		2.05	8.183	-10.681	TRP 230, TRP 387, TRP 581, ASP 455.

interactions with Trp 581, Asp 455, Phe 696, His 232, Trp 192 and Trp 230. The docking results of all the 26 molecules in the active site of lanosterol synthase were shown in Table 10.

All these results shows the presence of aromatic/substituted aromatic groups, charged polar groups, aliphatic cyclic/acyclic groups and aromatic or heteroaromatic groups enhances the activity of these compounds towards lanosterol synthase enzyme. Ligand 16 was selected as the reference structure for the designing of new molecules.

The newly designed compounds structure and their feature were listed in table 11. From the results the predicted activities of new ligands were in

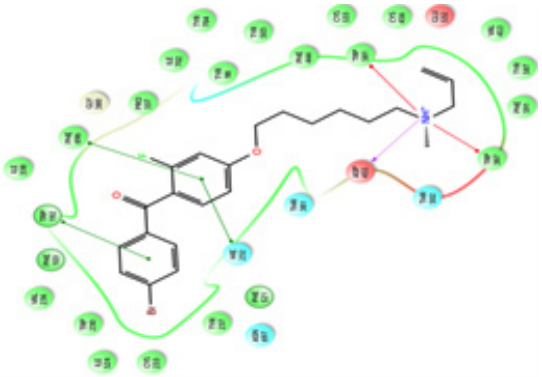

Fig.5: Reference ligand $R_0$48-8071

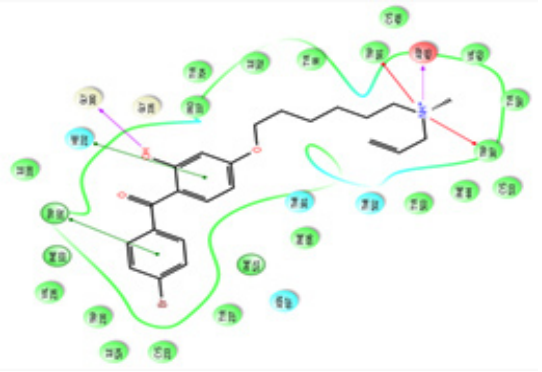

Fig. 6: Compound 8

Table 12. Prediction of drug-likeness of pharmacophore hits using qikprop simulation [23]

(Range 95% of drugs)

New ligand	Stars	Molecular weight[a] (g/mol)	Molecular Volume[b] (A^0)	PSA[C]	HB[d] donors	HB[e] acceptors	Rotatable bonds[f]
1	0	291.433	1157.595	47.625	1	4.250	12
2	0	304.431	1142.727	45.878	0	6.750	8
3	0	338.876	1175.044	47.353	0	6.750	8
4	0	383.327	1198.707	46.981	0	6.750	8
5	0	322.877	1173.287	17.375	0	4.750	8
6	0	324.893	1196.676	18.133	0	4.750	8
7	1	296.839	1069.583	18.354	0	4.750	7
8	0	296.839	1073.520	17.875	0	4.750	6
9	0	347.682	1005.227	28.123	1	4.250	6
10	0	347.682	1005.572	28.144	1	4.250	6

A * indicates violation of the 95% range (0 – 5.)

a - Molecular weight of the molecule (130.0 – 725.0)

b - Total solvent-accessible volume in cubic angstroms using a probe with a 1.4 Å radius (500.0 – 2000.0).

c - Van der Waals surface area of polar nitrogen and oxygen atoms and carbonyl carbon atoms (7.0 – 200.0).

d - Number of hydrogen bond donors (0.0 – 6.0).

e - Number of hydrogen bond acceptors (2.0 – 20.0).

f - Number of rotatable bonds (0 – 15).

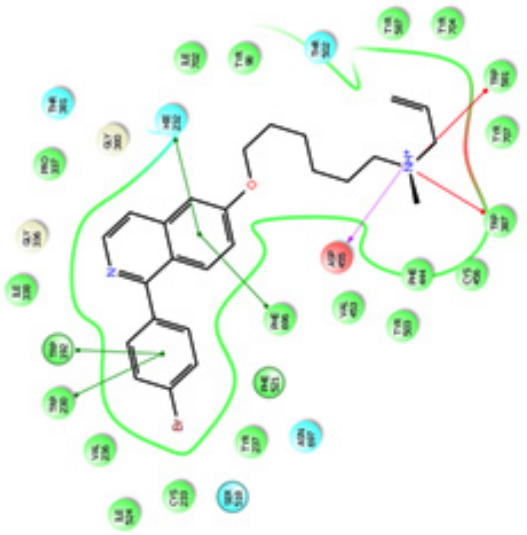

Fig.7: compound 16

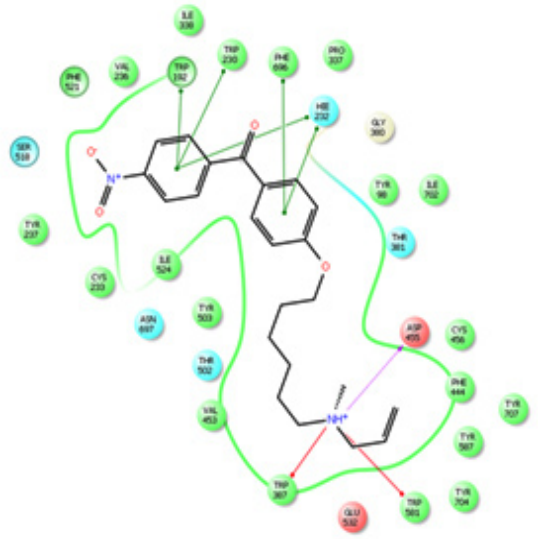

Fig. 8: compound 1

Table 13: Calculation of physicochemical properties using qikprop simulation[23]

(Range 95% of drugs)

New1	QPlog P(o/w)[a]	QPlogS[b]	QPPCaco[c]	QPlog HERG[d]	QPPMDCK[e]	% Human oral absorption
1	3.923	-3.903	581.701	-6.350	304.718	100
2	2.172	-1.506	181.319	-6.914	95.626	80.086
3	2.559	-2.145	158.887	-6.836	192.934	80.323
4	2.756	-2.463	171.455	-6.952	223.567	83.070
5	3.975	-3.194	513.098	-7.092	726.558	100
6	4.063	-3.515	513.541	-7.072	682.924	100
7	3.336	-2.436	554.159	-6.986	789.968	95.584
8	3.281	-2.573	513.107	-6.698	726.549	90.113
9	3.207	-2.817	300.977	-6.576	1010.670	90.083
10	3.211	-2.834	301.270	-6.590	1018.838	90.113

A * indicates violation of the 95% range.
An M indicates MW is outside training range.
QPlogP (o/w) —— Predicted octanol/water partition coefficient. (–2.0 – 6.5)
QPlogS —— Predicted aqueous solubility, log S. S in mol dm^{-3} is the concentration of the solute in a saturated solution that is in equilibrium with the crystalline solid. (–6.5 – 0.5)
QPPCaco —— Predicted apparent Caco-2 cell permeability in nm/sec. Caco-2 cells are a model for the gut blood barrier. QikProp predictions are for non-active transport. (<25 poor, >500 great)
QPlogHERG — Predicted IC50 value for blockage of HERG K+ channels. (below –5)
QPPMDCK —— Predicted apparent MDCK cell permeability in nm/sec. MDCK cells are considered to be a good mimic for the blood-brain barrier. QikProp predictions are for non-active transport. (<25 poor, >500 great)
Percent Human- Oral Absorption ——— Predicted human oral absorption in GI. (>80% is high <25% is poor)

the range of 8.06-8.29. The docking results of newly designed molecules in the active site of lanosterol synthase were shown in Table 11. These compounds showed significant docking score indicates that they can be used as LSS inhibitors. Qik prop can predict the toxicity and side effect of the ligand. ADMET calculation was performed using Qik prop for the newly designed molecules and the properties were shown in Table 12 and 13.

CONCLUSION

As per the above results the newly designed compounds showed fitness score higher than 2 and have good predicted pIC50 values in the range of 8.068-8.290. The docking score of all these compounds were larger than the reference ligand $R_0$48-8071 (docking score of R048-8071 was -10.309 kcal/mol). Insilico ADME/Toxicity analysis of these compounds showed promising results. Hence these ligands were selected for invitro and invivo studies to prove its efficacy as potential drugs in treating hypercholesterolemia.

REFERENCES

1. David, k.; *J.Natr.***1987**, *117*, 1330-1334.
2. U, Ravnskov.; *An Int. J.Med.* **2002**, *95*, 397-409.
3. Demierre,M.F.; Higgins, P.D.; Gruber, S.B.; Hawk, E.; Lippman, S.M. *Natr. Rev. Cancer.* **2005**, *95*, 930-942.
4. Chan,k.k; Oza,A.M.; Siu,L.C. *Clin.Cancer Res.***2003**,*9*,10-19.
5. Kasiske, B.L.; Wanner. C.; O'Neill. W.C. *Am. J. Cardiol.* **2006**, *97 [suppl]*, 82C-85C.
6. Pedersen,T.R.; Tobert,J.A. *A reappraisal.Drug Saf.***1996**,*14*,11-24.
7. Morand,O.H.; Aebi,J.D.; Dehmlow,H; ji,Y.H.; Gains.N.; et al. *J. Lipid Res.***1997**,*38*,373-390.
8. Bernhard,E.; Ralph,B.; Peter,M.; Roland,M.; Michael,M. *J.Lipid Res.***1997**,*38*,564-575.
9. Michael,M.; Peter,M.; Roland,M.; Bernhard,E. *J.Lipid Res.***1996**,*37*,148-158.
10. George,R.B.; David,M.H.; Elaine,S.E.S.; David,S.C.; et al. *J.Med.Chem.***1999**,*42*,1306-1311.
11. Armin,R.; Francis,M.; Brigitte,D.A.; Martine,S.; et al. *Biochem. Biophy. Res. Commun.* **2004**,*315*,247-254.
12. Rie,T.; Tanja,S.G.; Brigitte,D.A.; Jorg,B.; et al. *Lett.Natr.***2004,***432*,118-122.
13. Rie,T.; Yuichi,S.; Akito,N.; Masaaki,S.; et al. *Bioorg.Med.Chem.Lett.* **2005**, *15*, 159-162.
14. Hiroshi,T.; Satoshi,O. *Pharmacol.Therapt.* **2007**,*115*,375-389.
15. Mark,M.; Muller,P.;Maier,R.; Eisele,B.*J. Lipid Res.* **1996**,*37*,148-158.
16. Henrietta, D.; Johannes,D.A.; Synese,J.; Yu-Hua, Ji.; Elisabeth,M.V.M.; Jacques,H.; Oliver,H.M. *J.Med.Chem.***2003***,46*,3354-3370.
17. Dixon,S.L.Smondyrev,A.M.; Rao,S.*Chem.Biol. Drug.Des.***2006**,*67*,370-372.
18. Teli,M.K.; Rajanikant,G.K. *J.Enzyme.Inhib. Med.Chem.***2011**,*26*,1-13.
19. http://www.rcsb.org/pdb
20. Schrodinger suit **2009** Protein Preparation Wizard; Epik version 2.0; Impact version 5.5. Schrodinger, LLC, New York.
21. Friesner,R.A. et al.*J.Med.Chem.***2004**,*47*,1739-1749.
22. Friesner,R.A.; et al.*J.Med.Chem.***2006**,*49,*6177-6196
23. Schrodinger suit **2010** Protein Preparation Guide, Site Map 2.4; Glide Version 5.6,Lig Prep 2.4, Qik Propn3.3, Schrodinger, LLC, New York, NY,**2010.**